

SIMULATION OF STRONG-MOTION DISPLACEMENTS USING SURFACE-WAVE MODAL SUPERPOSITION

BY HENRY J. SWANGER AND DAVID M. BOORE

ABSTRACT

Synthetic seismograms constructed by addition of surface-wave modes in a layered half-space are compared to Cagniard-de Hoop calculations of Heaton and Helmberger (1977, 1978) and to ground displacement recordings near El Centro, California to examine the applicability of modal superposition as a means of simulating ground motion of possible engineering interest. Modal solutions of flat earth problems are desirable because of the modest cost involved and the versatility of the method in simulating extended sources and anelastic damping. *P-SV* and *SH* motions can be computed with almost equal ease. The comparisons show that in sedimentary structures surface waves can dominate ground displacement motion at epicentral distances of only a few source depths. Superposition of the higher modes often approximates quite well impulsive arrivals with analogies to refracted and reflected rays.

Ground displacement recordings of El Centro from the 1968 Borrego Mountain earthquake are modeled using a multi-layered geological structure and a source model based on independent studies. The gross character of the records appears to be insensitive to the details of the source. Both point sources and propagating sources with horizontal dimensions larger than half the epicentral distance give reasonable fits to the observed transverse motion. This insensitivity appears to be due to a complex interaction between rupture propagation and the surface-wave dispersion. By using the integrated El Centro accelerogram, which may have more reliable amplitude information than the Carder displacement record used in other studies, the moment is estimated to be 12×10^{25} dyne-cm. This is similar to values found from studies of teleseismic data.

INTRODUCTION

Motivated by the needs of earthquake engineering, the modeling and prediction of ground motions from earthquakes has become an important task for seismologists. Much of the early work ignored the effects of geological layering, but it is now clear that in many circumstances the layering has a significant influence on the motions. A number of methods have been developed to deal with the complications due to geological structure; these range from the approximation of the response of local sedimentary columns by vertical plane-wave propagation through a stack of layers (e.g., Joyner and Chen, 1975 and references therein) to the solution of the complete wave propagation from source to receiver in a multilayered medium. Solutions to the latter problem are usually obtained from generalized ray methods (e.g., Helmberger and Malone, 1975) or from direct frequency domain integration (Apsel *et al.*, 1977; Herrmann, 1977; Wiggins *et al.*, 1977). The generalized ray method can be inexpensive, but is poorly suited to problems with many layers and cannot easily account for attenuation except in an *ad hoc* manner. On the other hand, the frequency domain method can handle attenuation and a large number of layers, but at a relatively high price (although future generations of computers should reduce this to the point where the method is very practical). A compromise which we feel deserves attention is the use of superposition of surface-wave modes. Although an incomplete description of the motion, modal superposition is suggested by numerical and observational studies. These show that for shallow sources in typical earth

structures surface waves dominate the ground motion at moderate distances, on the order of tens of km, and at periods greater than 1 or 2 sec (Hanks, 1975; Herrmann, 1977; Herrmann and Nuttli, 1975a, b; Kawasaki, 1977; Trifunac, 1971).

Synthetic seismogram construction using modal superposition has a number of attractive features. The method has been widely used in studies of teleseismic waves, and therefore the details of the method have been worked out and efficient programs to compute the basic dispersion parameters are readily available. The dispersion parameters and eigenfunctions need only be computed once for the layered model to permit time-domain synthesis for any type and depth of source, azimuth, or epicentral distance. The time-domain synthesis is very simple in practice and the cost is negligible in most cases. The separation of source and media dependencies of the response allows for interpretation of the relative importance of source depth and near-site structural response. Furthermore, it is easy to extend the point source solutions to those from extended sources. Finally, in common with the frequency domain integration methods, modal superposition has the advantage over generalized ray methods that the number of layers is not a practical limitation—all interbed multiples are included—and *P-SV* solutions can be obtained almost as easily as *SH* motion, without significant increases of cost or error. In spite of these benefits however, modal superposition has drawbacks. It gives only an approximation to the total motion, and we have been unable to find an *a priori*, quantitative measure of the adequacy of the approximation. This seems to depend on epicentral distance, source depth, frequency, and the details of the layered model. Obvious examples where modal superposition is inadequate are when no surface layers exist, in which case there are no *SH* normal modes (this is clearly an extreme case, but illustrates the point), and when the source is so deep relative to the epicentral distance that the motion is dominated by energy with very high horizontal phase velocities. It may be possible to use modal superposition in this latter case if leaking modes are included (Laster *et al.*, 1965) but to retain the advantages of simplicity we have considered only normal modes in this paper.

In order to explore surface-wave superposition for the synthesis of ground motions, we have studied the displacement records from several earthquakes in or near the Imperial Valley of California. The sediments in this valley are remarkably flat lying and form a prominent wave guide (Biehler *et al.*, 1964). The records have been previously modeled with generalized ray methods (Heaton and Helmberger, 1977, 1978) providing us with a check of the modal superposition method. As we will see, the comparison is very good.

SURFACE-WAVE COMPUTATIONAL METHODS

The synthesis method is not new and will be only briefly described. For each mode, phase and group velocities, the amplitude response function, eigenfunctions at the midpoint of each potential source layer, and ellipticity (for Rayleigh waves) are obtained for a representative sample of frequencies. The increase of modes with frequency imposes a practical upper limit of about 1 Hz in simulations presented in this paper. Anelastic attenuation can be included using the methods of Anderson and Archambeau (1964).

Horizontally propagating sources of finite vertical extent are treated by a combination of analytical integration over depth and the collapse of extended segments into point sources by a generalization of Ben-Menahem's directivity function (Ben-Menahem, 1961). We have used a program based on Harkrider (1964, 1970) for

computation of the basic dispersion parameters. For a particular synthetic seismogram, appropriate combinations of the above parameters and the source-station distance and geometry are interpolated (using spline functions) to obtain a complex Fourier displacement spectrum at equally spaced frequencies. Fast Fourier transformation gives the time history.

COMPARISON WITH COMPLETE SOLUTIONS

Heaton and Helmberger (1977 and 1978) have modeled the transverse components of ground displacement from two earthquakes in the vicinity of the Imperial Valley,

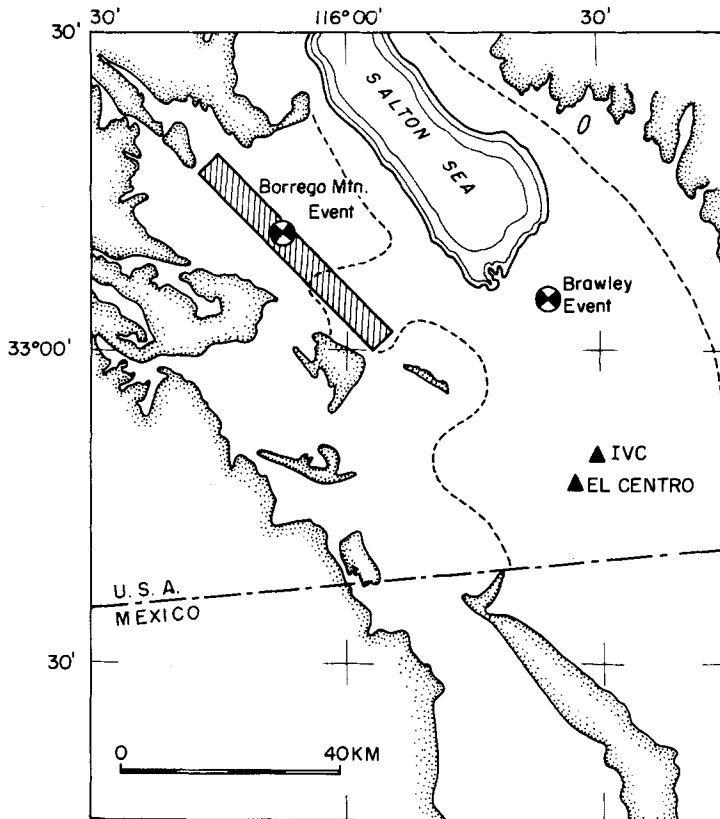


FIG. 1. Map of study area, showing epicenters of the 1968 Borrego Mountain and 1976 Brawley earthquakes and location of recording sites (IVC was installed after 1968). Most of the aftershocks along the trend of faulting in the 1968 event fell within the rectangular area shown (Hamilton, 1972). The stippled pattern marks areas underlain by pre-Tertiary crystalline rock and the dashed line marks the approximate ancient shoreline of Lake Coahuila. Base map modified from Chart I, Biehler *et al.* (1964).

California (see Figure 1 for geometry). They have used enough rays so that their synthetics can be considered the complete solution for the record lengths shown. Their models for the 1968 Borrego Mountain earthquake recorded at El Centro were based on a simplified geological structure consisting of one layer over a half space (Table 1). We computed surface-wave synthetics for one of their models in which a point source was located at a depth of 6 km (Figure 2). The acausal surface-wave synthetics gave a poor fit to the direct arrival (as expected) but closely matched most of the rest of the motion. Acausality is a characteristic of all modal contribu-

tions, but, unlike spherical earth normal modes, superposition of all flat earth modes cannot remove these fictitious contributions. The disagreement late in the record is found in a number of our comparisons, although it may be due to the presence of leaking modes in the complete solution which have high-phase velocities and low-group velocities; it may also result from the asymptotic approximations made in the two methods.

The good overall fit of the approximate surface-wave solution to the complete solution is not surprising considering the oscillating, wave guide-like character of the ground displacement. Note that most of the motion corresponds to the fundamental Love wave mode and that the source exciting these Love waves is below the

TABLE 1
EL CENTRO STRUCTURE USED BY HEATON AND HELMBERGER
(1977)

Thickness (km)	P Velocity (km/sec)	S Velocity (km/sec)	Density (gm/cc)
2.9	—	1.5	1.5
—	—	3.3	2.5

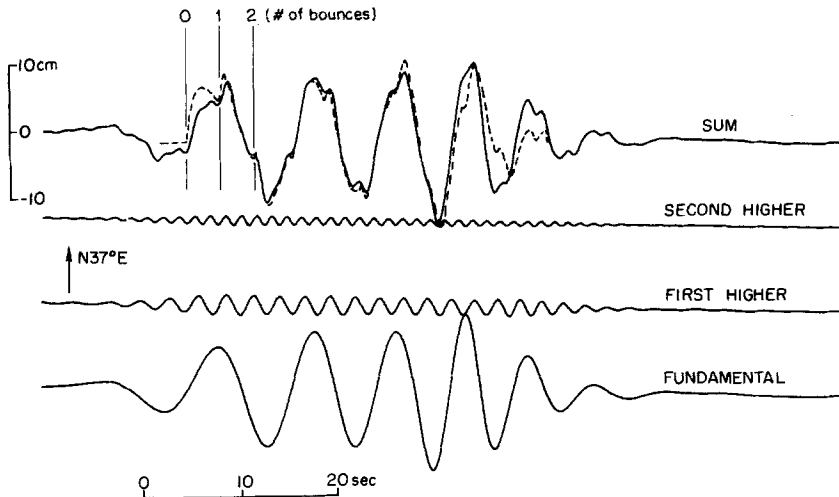


FIG. 2. Comparison of Love wave synthetic ground displacements (solid line) with Heaton and HelMBERGER's model B42 of the 1968 Borrego Mountain earthquake (dashed line). The source depth and epicentral distance were 6 and 60 km, respectively, and the moment was 6.7×10^{25} dyne-cm. The separate modal contributions are shown in the *bottom* three traces. Arrival times for the direct ray and the first two multiples are shown.

layer, so that none of the geometric ray paths to the station can have apparent velocities in the range of the Love wave phase velocities. As discussed by HelMBERGER and MALONE (1975), the trapped modes are set up by a diffraction or tunneling of energy into the layer.

The Brawley earthquake provides a more interesting test of the surface-wave synthesis method than did the Borrego Mountain event. Heaton and HelMBERGER's velocity model was more complicated, consisting of three layers over a half-space (Table 2) and the synthetics, which were a good match to the data, looked less like surface waves. The ratio of epicentral distance-to-source depth was also less, 4.8 rather than 10. The surface-wave synthetics (Figure 3) are not as good a fit to the complete solution as they were before, but they do reproduce much of the record's

character, including the discrete looking arrivals associated with the direct wave and the first multiple in the sedimentary section. In this case the higher modes were essential in defining the shape of the wave form.

That higher modes are not necessarily needed to give a body wave-like seismogram is shown by the example in Figure 4, taken from Kawasaki (1978). The source was

TABLE 2
IMPERIAL VALLEY STRUCTURE USED BY HEATON AND HELMBERGER
(1978)

Thickness (km)	P Velocity (km/sec)	S Velocity (km/sec)	Density (gm/cc)
0.95	2.0	0.88	1.8
1.15	2.6	1.5	2.35
3.8	4.2	2.4	2.6
—	6.4	3.7	2.8

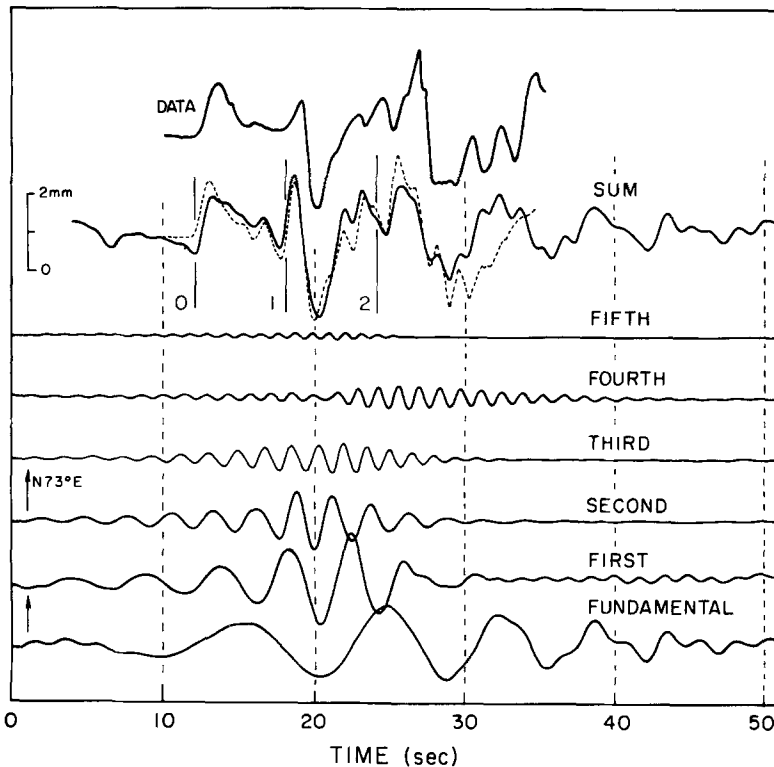


FIG. 3. Comparison of Love wave synthetic ground displacements with Heaton and HelMBERGER's model of the 1976 Brawley earthquake as recorded at IVC, 33 km from the epicenter. A vertical strike-slip point source buried at 6.9 km was used. The equivalent source time function was a symmetrical triangle with a base of 1.5 sec. The moment was 3.2×10^{23} dyne-cm. For comparison, the top trace gives the data. The arrival times are for the direct arrival and the first two multiples in the sedimentary section. In the traces shown here there is sometimes a small amount of spurious motion at the beginning and end of the records; this is due to the periodicity of the Fourier transform.

buried at 10 km in a 30-km thick layer and the epicentral distance was 301 km. The gradual increase of motion at the beginning of the fundamental mode solution, similar in appearance to the head wave refracted from the base of the layer, is due to arrivals coming from the long-period branch of the dispersion curve. The short-

period branch contributes a sharply defined phase, which at this large epicentral distance coincides in time with the direct and wide angle reflections.

With confidence gained from the comparisons above, in the next sections we apply the surface-wave synthesis method to a further study of the El Centro recording of the Borrego Mountain earthquake.

APPLICATION TO BORREGO MOUNTAIN EARTHQUAKE

There are several reasons that the El Centro recording of the April 9, 1968 Borrego Mountain earthquake is a convenient subject for further study of the modal

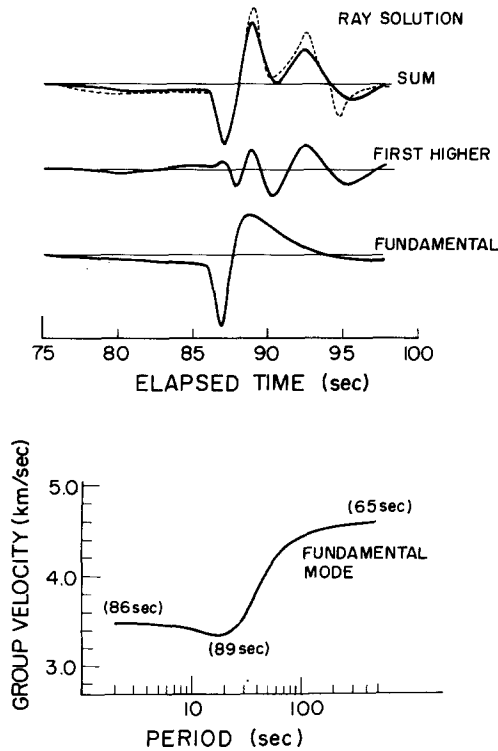


FIG. 4. (a) Comparison of mode (solid) and ray (dashed) solutions for the SH ground displacement at 301 km from a source buried 10 km in a 30-km thick layer. The shear velocities of the layer and half space are 3.5 and 4.6 km/sec, respectively. The source time function had a 2-sec rise time. (b) Group velocity for the model above: Group arrival times for the end points and the minimum of the curve are shown in parentheses for comparison with the wave form in (a). Both (a) and (b) are modified from Figures 23 and 26 in Kawasaki (1978).

synthesis method: surface waves clearly dominate the ground displacement, the geological layering near the site is uniform laterally, and independent studies of the velocity structure of the sediments have been made (Biehler *et al.*, 1964). Furthermore, we were curious as to how well the record would be fit using these independently determined velocities; in their study of the record, Heaton and Helmberger (1977) used a simple layer over a half-space with properties chosen to match the periodicity of the record.

Our study of the El Centro record is intended to illustrate the versatility of seismogram constructions using modal superposition and to reveal the role of surface waves in ground motions in sedimentary basins. We do not claim to have improved

on previous workers' descriptions of the faulting process. This earlier work has guided our choice of the fault models considered in our synthetics.

The crustal structure in the vicinity of the earthquake source and the recording station at El Centro is different, and this would seem to cause difficulties in the modeling (which assumes plane layers). Tables 3 and 4 show our estimates of the velocity structure in the two regions. In both cases the velocities in the lower crust and upper mantle are guided by the results of Thatcher and Brune (1973). The structure in the epicentral region was adapted from Hamilton (1970) and the velocities in the vicinity of El Centro were based on Biehler *et al.* (1964). In the latter case the velocities shown are the ones used in the synthesis but they correspond to a part of the Imperial Valley toward the epicenter from El Centro, rather than the local area of El Centro itself. They were chosen in this way in an attempt to compensate for the laterally changing thickness of the Imperial Valley.

TABLE 3
STRUCTURE NEAR 1968 BORREGO MOUNTAIN EARTHQUAKE
EPICENTER

Thickness (km)	P Velocity (km/sec)	S Velocity (km/sec)	Density (km/sec)
0.8	2.4	1.4	1.5
0.8	3.5	2.0	2.0
2.9	5.0	2.9	2.3
7.0	6.1	3.5	2.6
8.5	7.1	4.1	2.8
—	7.8	4.5	3.1

TABLE 4
STRUCTURE USED IN CALCULATIONS

Thickness (km)	P Velocity (km/sec)	S Velocity (km/sec)	Density (km/sec)
0.25	1.7	1.0	2.0
0.30	2.1	1.2	2.2
1.35	2.4	1.4	2.2
0.95	3.3	1.9	2.4
1.65	4.3	2.5	2.5
7.0	6.2	3.6	2.9
8.5	7.1	4.1	3.0
—	7.8	4.5	3.1

The significant differences in the two structures in Tables 3 and 4 are at depths shallower than about 8 km, while the distribution of aftershocks of magnitude 3.5 and greater suggests that the major part of slip occurred at depths below 6 km (Hamilton, 1972). Heaton and Helmberger (1977) justify the use of an El Centro type structure on the basis of ray arguments which suggest that the dominant part of the motion is composed of multiple bounces in the layer at progressively greater distances from the station. Their arguments seem quite reasonable for a ray approach and should be as justifiable in a modal approach. The contributions which will probably strongly sense the structure above the source will be the contributions with low group velocities. These parts of the motion are those whose excitation for a buried source is relatively low, or are contributions which would not be included in the modal analysis anyway, the so-called "leaking modes". For the distances and source depths to be considered here, it seems reasonable to assume that the characteristics of the motion at El Centro will be only weakly dependent on the near surface structure at the epicenter.

Before proceeding, we emphasize that the velocity structure in Table 4 was chosen before any synthetic seismograms were computed. No alterations of the model were made to improve the fit to the data.

Dispersion parameters for the four lowest Love- and Rayleigh-wave modes were computed. These correspond to all the trapped modes for periods greater than about 2.5 sec, and they are the dominant contributions at periods down to about 1.5 sec. At shorter periods higher modes than the third exist, but they contribute little to the synthetic seismograms.

The basic point source Love-wave synthetic seismogram for a 8-km deep source at 66 km from the epicenter is shown in Figure 5. The depth corresponds to the mean depth of aftershocks with magnitude of 3.5 or larger (Hamilton, 1972). The

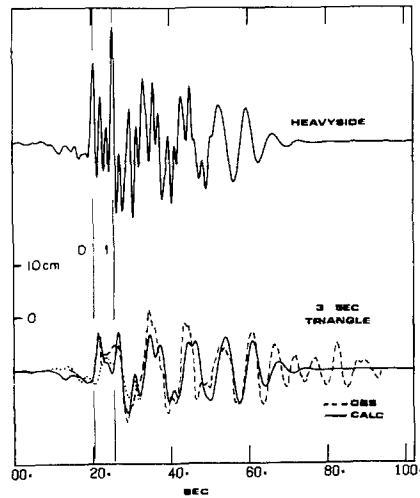


FIG. 5. Love wave synthetic ground displacements for a model of the 1968 Borrego Mountain earthquake in which a vertical, strike-slip point source was buried at 8 km in the structure given in Table 4. The moment was 6.3×10^{25} dyne-cm and the epicentral distance was 66 km. The top trace assumed a source with a step function; the bottom trace corresponds to a source time function whose derivative was a symmetrical triangle of 3 sec duration. The moment was taken from Wyss and Hanks (1972), a moment of 9×10^{25} dyne-cm would give a better fit to the motion after about 30 sec. The data (dashed) are from Heaton and Helmberger (1977). As discussed in the summary section, the amplitude scale may underestimate the true amplitudes by about 30 per cent. The two vertical lines give the arrival times of the direct ray and the ray with a multiple bounce between the surface and the top of the layer with 3.6 km/sec S velocity. Reflections from the two interfaces below the source arrive within 0.2 sec of the times indicated. Eliminating the velocity contrasts in the layers below the source leads to the motions shown by the dotted line.

moment of 6.3×10^{25} dyne-cm is that found by Wyss and Hanks (1972) from field evidence and teleseismic body waves. The top trace corresponds to a source in which the relative offset of the two sides of the fault occurs instantaneously, and the bottom trace is the result of convolving the top trace with a 3-sec triangle function to account for the smoothing effect of rupture propagation and the finite rise time of the source-time function. The dashed line is the transverse displacement that Heaton and Helmberger (1977) obtained by rotating the Carder Displacement meter records after removing the instrument response (Heaton and Helmberger's displacements will be used throughout this paper as the most useful representation of the El Centro ground motion). Figure 5 shows that a reasonable fit to the data is given by a simple source model and a velocity structure and moment taken from previous studies. For this earthquake the overall character of the ground displacement at El

Centro is determined by the geological structure and has very little to do with the source characteristics (triangle filters of 2 and 4 sec gave similar results). This isn't to say that the source is necessarily simple, but rather that the source duration as perceived at El Centro is short compared to the resonant periods of the structure.

The surface-wave method predicts early phases which look remarkably like body waves and, as shown in the figure, the arrival times of these motions correspond to ray arrivals. In the model used in the figure, the direct wave and the reflections and refractions from the intermediate layer and the base of the crust arrive within 1 sec of one another, and it is therefore difficult to associate the motion with a particular ray. To aid in our understanding of the initial motions, we ran the modal solution for a velocity structure for which the layer below the sedimentary column was extended to infinite depth, thereby putting the source into the half-space. The results (given by the dotted line) show that the initial arrival, and consequently the

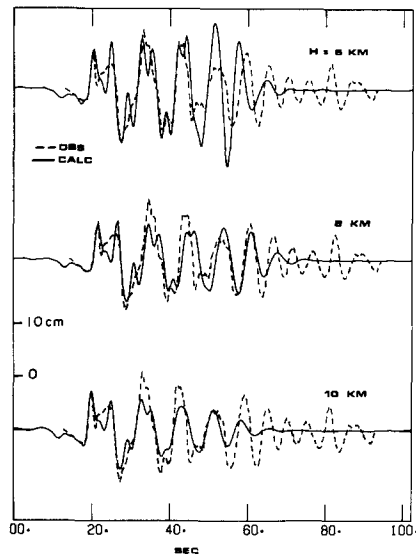


FIG. 6. Effect of depth on ground displacements for the same model used in Figure 5. Data are shown by dashed lines. Note the depth dependence on the relative amplitude between the first arrival and the later motions.

fit to the data, has been degraded, supporting Heaton and Helmberger's statement that the character of the initial part of the motion may be explained by diving rays.

Figure 6 shows the 3-sec triangle response for three different depths. The periodicity of the wave forms is not altered greatly from one depth to another, but the relative amplitudes of early and late parts of the recording change a great deal. Such observations might be used to better constrain source depth when velocity structure is well known. In this particular case a source depth of 8 or 9 km probably best fits the relative amplitudes throughout the record.

As shown above, the transverse component of ground displacement can be modeled by Love waves from a point source. A more realistic model of faulting, of course, allows for rupture over an extended source. By suitable alterations of the spectrum, the surface wave computations can account for rupture propagation. To test the method, we repeated one of Heaton and Helmberger's extended source calculations, using the layer-half space structure in Table 1. They added up contributions from small fault segments in order to model a rupture of finite vertical

extent which started at a point and spread circularly over the fault plane until the edges of the fault were encountered. Our fault is simpler, corresponding to a propagating line source at the hypocentral depth. In spite of these differences in fault complexity, the comparison between the two methods is good (Figure 7). A feature of note is the enhancement of the first peak in the motion (compare Figures 2 and 7). Although, as shown earlier, diving rays can lead to a sharp first peak, they are not required if we allow for fault propagation.

We next applied our method to a study of the effects of rupture velocity on the ground displacements for a finite fault in the multilayered El Centro structure (Table 4). Guided by the aftershock distributions (Allen and Nordquist, 1972; Hamilton, 1972) and the results in Figure 6, we chose a rectangular fault extending from 5 to 11 km depth, with bidirectional rupture starting at the epicenter (66 km

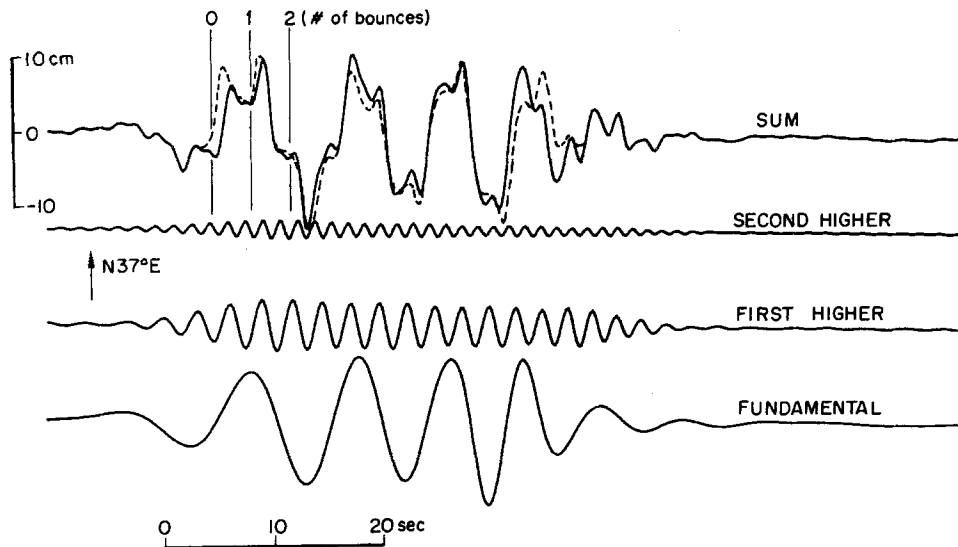


FIG. 7. Comparison of Love wave synthetic ground displacement with Heaton and Helmberger's model BNOR1 of the 1968 Borrego Mountain earthquake. A source at 6 km depth propagated 6 km and 5 km toward and away from El Centro, respectively, at a velocity of 2.5 km/sec. The moment was 6.9×10^{25} dyne-cm. The structure model is given in Table 1. Heaton and Helmberger distributed their source between 3.5 and 8.5 km depth and assumed a rupture which spread out circularly from the epicenter.

from El Centro). The rupture was assumed to propagate 27 and 10 km toward and away from El Centro, respectively. The slip, rupture velocity, and rise time were constant over the fault area. The Love-wave motions for the transverse component (as defined by the perpendicular to the line from the epicenter) are shown in Figure 8. A range of rupture velocities from 0.6 to 0.9 β was used, where β is the shear velocity in the layer in which the fault was embedded. The rise time was weakly coupled to rupture velocity, leaving rupture velocity and moment as the independent parameters. The moments were determined by scaling the maximum absolute displacements of the synthetics to the data.

From considerations of directivity (e.g., Boore and Joyner, 1978) we would expect the frequency content to decrease as rupture velocity decreases. The results in Figure 8 are consistent with this. In particular, note the smearing of the double peaks near the beginning of the record; this would seem to eliminate the slower rupture velocities. Although it may be objected that the surface-wave method gives

a questionable prediction of the first motions, Heaton and Helmberger (1977, Figure 10) observed a similar smearing of the double peak in their simulation of an extended fault with a range of rupture velocities. It is commonly thought that the determination of rupture time (and thus, rupture velocity if the fault length is known) from a single station is difficult because of the tradeoff with rise time, but in Figure 8 it doesn't seem that decreasing the rise time will compensate for the slow rupture velocity. The rupture time/rise time tradeoff is easily demonstrated for a uniform whole space, but apparently when layers are added the various modes (or rays) making up the motion are affected differently by the rupture so that in some cases a single station recording may be able to resolve the tradeoff, especially if the structure is known.

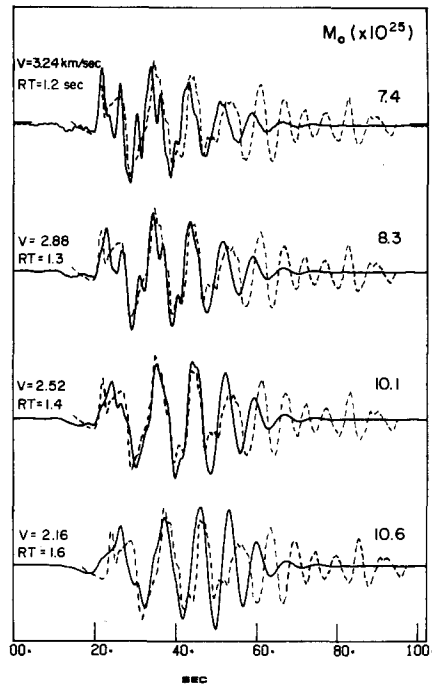


FIG. 8. Effect of rupture velocity on the ground displacements for the structure in Table 4. For comparison, the data are shown by dashed lines. A weak dependence of rise time on rupture velocity was assumed. The rupture velocities were chosen as 0.6, 0.7, 0.8, and 0.9 of the shear velocity of the layer in which the source was embedded (3.6 km/sec). The fault propagated 27 and 10 km toward and away from El Centro, respectively, and it extended from 5 to 11 km depth.

Choosing a rupture velocity $V = 0.8 \beta$ on the basis of Figure 8, we computed the Rayleigh-wave contributions for the propagating source. This and the Love-wave motion were combined into the three components shown in Figure 9a. On the vertical component the fit to the data is fairly good for about 15 or 20 sec and considerably better than that using a point source (Figure 9b). The radial synthetic has about the right amplitudes in the first 20 to 30 sec after the initial *S* arrival but has a poor phase match. This is not surprising since what we call the radial component of motion is defined with respect to the epicenter; it is a mixture of radial and transverse motion for radiation from most of the fault. In fact, the Love- and Rayleigh-wave contributions to this component are about equal in amplitude. Therefore any phase error in either could distort the combined motion. To a large

extent the increase of amplitude on the radial and vertical components compared to that for the point source is a result of changes in the geometrical spreading and the Rayleigh wave radiation pattern as the fault propagates toward the station. The large amplitude, late-arriving motions seen in the records (starting at about 55 sec) cannot be explained by a reasonable source and plane-layered model; as suggested by Heaton and Helmberger (1977), they are probably due to lateral reflections and refractions from the edges of the Salton Trough.

None of the calculations in this paper included attenuation. To check the significance of this assumption, the propagating source calculation used in Figure 9a was

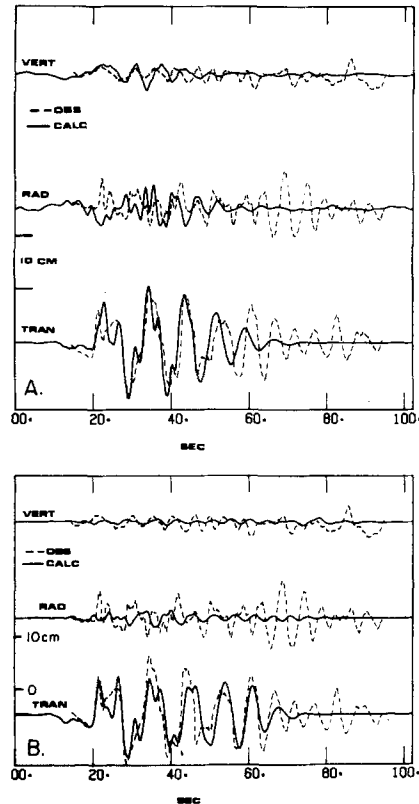


FIG. 9. (a) Three components of ground displacement for the propagating source used in Figure 8, with rupture velocity of 2.88 km/sec. The moment was 8.3×10^{25} dyne-cm. (b) Three components of ground displacement for the point-source model used in Figure 5. Rayleigh and Love waves were used in the synthetics in both (a) and (b).

repeated with shear Q' 's ranging from 25 at the surface to 75 at the base of the sediments. No attenuation was included in the material below the sediments. The wave forms were similar to the perfectly elastic calculations, but the amplitudes in the later parts of the record were reduced slightly (10 per cent for the peak motion).

EFFECT OF RUPTURE VELOCITY ON AMPLITUDES

Both we (Figure 8) and Heaton and Helmberger (1977) found that for a given moment the peak amplitudes were not a strong function of rupture velocity. This surprised us, because the rupture velocities ranged up to 0.9 of the shear velocity in the source layer and were equal to the Love-wave phase velocities at frequencies

within the bandwidth of the output motion. For body waves in a uniform whole space, the amplitude of the motion is very sensitive to the rupture velocity when it is close to the apparent velocity, along the direction of fault rupture, of the waves radiated from the source: a factor of 5 increase is found going from $V = 0.6 \beta$ to $V = 0.9 \beta$. To understand this difference in behavior, we used a model similar to that in Figure 7 but with unidirectional faulting of 11 km toward El Centro from the hypocenter (Heaton and Helmberger's BNOR5). The peak amplitudes for a number of phase velocities are shown in Figure 10a. Clearly a strong dependence on rupture velocity does exist for the slower velocities, but a plateau forms at higher velocities.

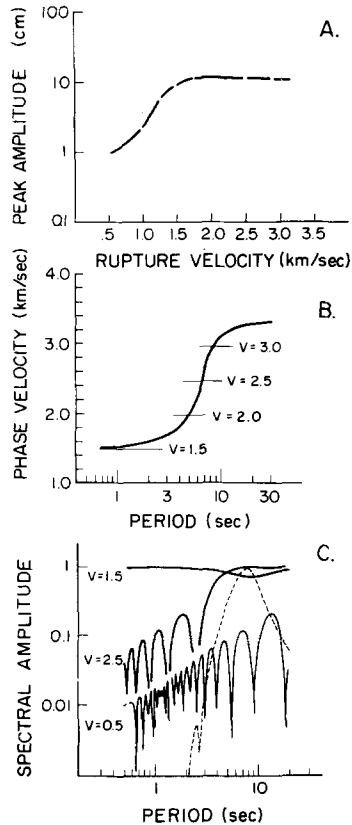


FIG. 10. (a) Dependence of peak amplitude on rupture velocity for a source similar to that in Figure 7, except with 11 km of unidirectional rupture toward El Centro. (b) Fundamental mode phase velocity curve for the structure in Table 1. The values of phase velocity which equal $V \cos \theta$ are shown by the short lines ($\theta = 8^\circ$). (c) Factorization of the fundamental mode spectral excitation into parts which do and do not depend on rupture propagation (solid and dashed, respectively). The peak of the dashed curve is normalized to unity. The solid curves are not normalized.

What we are seeing is a complex interaction of mode excitation, rupture length, and frequency-dependent phase velocities. The amplitude spectrum of the motion is given by a product of several frequency-dependent terms, one involving the eigenfunctions and spectral excitations for a point source, and another giving the modifications for rupture propagation. The latter is given to first order by the well-known equation

$$R = |\sin \chi / \chi|$$

where $\chi = (\pi L/T)[1/V - \cos \theta/C(T)]$ and $L =$ rupture length, $T =$ period, $V =$ rupture velocity, $\theta =$ azimuth from the direction of rupture propagation to the station, and $C(T)$ is the period-dependent phase velocity. Figure 10b shows the fundamental mode phase velocities (the fundamental mode dominates the motions), and Figure 10c shows the $\sin \chi/\chi$ contribution to the fundamental mode spectrum for rupture velocities of 0.5, 1.5, and 2.5 km/sec. For slow rupture velocities the $1/V$ term dominates χ , and as V increases the corner of the spectrum (off the plot to the right) moves steadily to the left with a resultant steady increase in the spectral excitation. When V is in the range of the phase velocities, things get more complicated. At the period for which $C(T) = V \cos \theta$, the excitation factor R becomes unity because $\chi = 0$. At longer periods χ can remain small (and R close to 1) if the fault length is sufficiently short. This has happened for the $V = 1.5$ km/sec case in Figure 10c, where a relatively flat excitation occurs over a wide-period band. If the fault length had been larger, the curve for $V = 1.5$ km/sec would have shown a peak for the shorter periods. Note that the $V = 2.5$ km/sec curve shows smaller excitation than does the $V = 1.5$ km/sec curve; this is because the phase velocity isn't equal to $V \cos \theta$ until a period of about 7 sec is reached.

The amplitudes of the output are determined by the product of R and the part of the excitation function not dependent on rupture propagation. The dashed line in Figure 10c shows the contribution for this latter term for the source used here (depth equal to 6 km). The excitation is peaked around 8 sec, and we would expect the ground motions for the $V = 1.5$ km/sec and 2.5 km/sec cases to be similar, as indeed they are. If the excitation given by the dashed line had been centered around 1 or 2 sec, the ground motion for $V = 1.5$ km/sec would have been considerably larger than for $V = 2.5$ km/sec.

Thus we see that the ground motion can be a sensitive function of rupture velocity, but depends on a complex interaction of the fault length, the detailed shape of the dispersion curve, and the part of the excitation function not dependent on the rupture.

SUMMARY AND DISCUSSION

Ground displacements recorded in sedimentary basins at several tens of kilometers from shallow earthquakes are often dominated by surface waves. This suggests that the synthesis of such motions be done using modal superposition. To test this, we compared the wave forms computed using modal superposition with the "complete" solutions reported by Heaton and Helmberger (1977, 1978) in their study of two earthquakes recorded in the Imperial Valley of California. The comparison was encouraging, even when the wave form was more pulse-like than oscillatory. Modal superposition was then used to study the El Centro recording of the 1968 Borrego Mountain earthquake. In many respects our conclusions are the same as those of Heaton and Helmberger (1977) who used a simplified geological structure chosen to fit the data. Our structure was taken from independent data and was selected before modeling began [note that in a later study, Heaton and Helmberger (1978) were able to model another Imperial Valley recording with an independently chosen geological structure]. The first 20 to 30 sec of the transverse component of motion at El Centro was fit equally well by a point source and by a source with bidirectional rupture at 2.9 km/sec on a 37-km long fault extending from 5 to 11 km depth with a rise time of 1.3 sec. The dimensions of the extended source were taken from aftershock studies. The vertical and radial components of motion were better fit by the propagating source.

A moment of 8×10^{25} dyne-cm was found from our extended source model. Heaton and Helmberger (1977) found an average moment of 7×10^{25} dyne-cm, Wyss and Hanks (1972) estimated it to be 6×10^{25} dyne-cm from field data and body-wave spectra, and Burdick and Mellman (1976) found 11×10^{25} dyne-cm from time domain comparison of the teleseismic body waves. For two reasons our value of 8×10^{25} dyne-cm should be raised to about 12×10^{25} dyne-cm; first, the neglect of attenuation leads to a 10 per cent overestimation of the wave amplitudes; second, the ground motion values to which we scaled our model results are probably underestimated by about 30 per cent. We used the values derived from Heaton and Helmberger (1977), using Carder Displacement readings, but as they pointed out these values are smaller than those obtained from a double integration of the accelerogram record. Other studies of ground motions obtained from Carder Displacement Meter and integrated accelerograms have found a scale difference between the two (Trifunac and Lee, 1974). Based on the ease with which the sensitivity of the Carder Displacement Meter can be changed (Cloud, 1964), we believe that the amplitudes of the ground motions from the accelerogram integrations are to be preferred in this case.

The greatest influence of rupture velocity was found to be on the early part of the seismogram. A smoothing of the double peak at the beginning was used as evidence against rupture velocities as low as 2.2 km/sec. The effect of the rupture velocity, however, is a complicated function of rupture length, source excitation, period-dependent phase velocities, and modal composition. The smoothing of the double peak would probably not occur if we had used a rupture length significantly smaller than we did.

Although the relatively flat-lying, deep sediments of the Imperial Valley form an ideal wave guide which enhances the surface-wave content of the ground motion, there are a number of other sites of interest to earthquake engineers—such as the sedimentary basins in which oil resources are found—for which surface waves may also dominate the motion, and in such cases the method of modal superposition will be a convenient, economical way to synthesize ground displacements for use in the analysis of the seismic hazard to engineering structures.

ACKNOWLEDGMENTS

We thank Shi-chen Wang for her assistance in the computations for the Brawley earthquake, and Bob Geller and Bob Herrmann for their critical reviews of the manuscript. This research was supported in part by the Division of Advanced Environmental Research and Technology, National Science Foundation, Grant NEV 75-05148.

REFERENCES

- Allen, C. R. and J. M. Nordquist (1972). Foreshock, main shock, and larger aftershocks of the Borrego Mountain earthquake, in *The Borrego Mountain Earthquake of April 9, 1968, U.S. Geol. Surv. Profess. Paper 787*, 16–23.
- Anderson, D. L. and C. B. Archambeau (1964). The anelasticity of the earth, *J. Geophys. Res.* **69**, 2071–2084.
- Apsel, R. J., J. E. Luco, and J. A. Orcutt (1977). Body wave and surface wave propagation in a multi-layered half-space, (abstract), *Abstracts with Programs, Geol. Soc. Am.* **9**, 381.
- Ben-Menahem, A. (1961). Radiation of seismic surface waves from finite moving sources, *Bull. Seism. Soc. Am.* **51**, 401–435.
- Biehler, S., R. L. Kovach, and C. R. Allen (1964). Geophysical framework of the northern end of the Gulf of California structural province, in *Marine Geology of the Gulf of California*, T. H. van Andel and G. G. Shor, Jr., Editors, *Am. Assoc. Petrol. Geologists Mem.* **3**, 126–143.
- Boore, D. M. and W. B. Joyner (1978). The influence of rupture incoherence on seismic directivity, *Bull. Seism. Soc. Am.* **68**, 283–300.

- Burdick, L. J. and G. R. Mellman (1976). Inversion of the body waves from the Borrego Mountain earthquake to the source mechanism, *Bull. Seism. Soc. Am.* **66**, 1485-1499.
- Cloud, W. K. (1964). Instruments for earthquake investigation, in *Earthquake Investigations in the Western United States 1931-1964*, D. S. Carder, Editor, *U.S. Dept. of Commerce Publ.* 41-2, 5-20.
- Hamilton, R. M. (1970). Time-term analysis of explosion data from the vicinity of the Borrego Mountain, California, earthquake of 9 April 1968, *Bull. Seism. Soc. Am.* **60**, 367-381.
- Hamilton, R. M. (1972). Aftershocks of the Borrego Mountain earthquake from April 12 to June 12, 1968, in *The Borrego Mountain Earthquake of April 9, 1968*, *U.S. Geol. Surv. Profess. Paper* 787, 31-54.
- Hanks, T. C. (1975). Strong ground motion of the San Fernando, California, earthquake: ground displacements, *Bull. Seism. Soc. Am.* **65**, 193-225.
- Harkrider, D. G. (1964). Surface waves in multilayered elastic media I. Rayleigh and Love waves from buried sources in a multilayered elastic half-space, *Bull. Seism. Soc. Am.* **54**, 627-679.
- Harkrider, D. G. (1970). Surface waves in multilayered elastic media. Part II. Higher mode spectra and spectral ratios from point sources in plane layered earth models, *Bull. Seism. Soc. Am.* **60**, 1937-1987.
- Heaton, T. H., and D. V. Helmberger (1977). A study of the strong ground motion of the Borrego Mt., California earthquake, *Bull. Seism. Soc. Am.* **67**, 315-319.
- Heaton, T. H. and D. V. Helmberger (1978). Predictability of strong ground motion in the Imperial Valley: modeling the M 4.9, November 4, 1976 Brawley earthquake, *Bull. Seism. Soc. Am.* **68**, 31-48.
- Helmberger, D. V. and S. D. Malone (1975). Modeling local earthquakes as shear dislocations in a layered half space, *J. Geophys. Res.* **80**, 4881-4888.
- Herrmann, R. B. (1977). Research study of earthquake generated SH waves in the near-field and near-regional field. Final report, contact DACW39-76-C-0058, Waterways Experiment Station, Vicksburg, Miss.
- Herrmann, R. B. and O. W. Nuttli (1975a). Ground-motion modelling at regional distances for earthquakes in a continental interior. I. Theory and observations, *Earthquake Eng. Struct. Dyn.* **4**, 49-58.
- Herrmann, R. B. and O. W. Nuttli (1975b). Ground-motion modelling at regional distances for earthquakes in a continental interior. II. Effect of focal depth, azimuth, and attenuation, *Earthquake Eng. Struct. Dyn.* **4**, 59-72.
- Joyner, W. B. and A. T. F. Chen (1975). Calculation of nonlinear ground response in earthquakes, *Bull. Seism. Soc. Am.* **65**, 1315-1336.
- Kawasaki, I. (1978). The near-field Love wave by the exact ray method, *J. Phys. Earth* (in press).
- Laster, S. J., J. G. Foreman, and A. F. Linville (1965). Theoretical investigation of modal seismograms for a layer over a half-space, *Geophysics* **30**, 571-596.
- Thatcher, W. and J. N. Brune (1973). Surface waves and crustal structure in the Gulf of California region, *Bull. Seism. Soc. Am.* **63**, 1689-1698.
- Trifunac, M. D. (1971). A method for synthesizing realistic strong ground motion. *Bull. Seism. Soc. Am.* **61**, 1739-1753.
- Trifunac, M. D. and V. W. Lee (1974). A note on the accuracy of computed ground displacements from strong-motion accelerograms, *Bull. Seism. Soc. Am.* **64**, 1209-1219.
- Wiggins, R. A., J. Sweet, and G. A. Frazier (1977). The Parkfield earthquake of 1966—a study of the dislocation parameters based on a complete modeling of elastic wave propagation (abstract), *EOS, Trans. Am. Geophys. Union* **58**, 1193.
- Wyss, M. and T. C. Hanks (1972). Source parameters of the Borrego Mountain earthquake, in *The Borrego Mountain earthquake of April 9, 1968*, *U.S. Geol. Surv. Profess. Paper* 787, 24-30.

DEPARTMENT OF GEOPHYSICS
 STANFORD UNIVERSITY
 STANFORD, CALIFORNIA 94305

Manuscript received February 8, 1978